Journal Pre-proofs

Electrospun fixed dose combination fibers for the treatment of cardiovascular disease

Lixiang Zhao, Mine Orlu, Gareth R. Williams

PII: S0378-5173(21)00230-1
DOI: https://doi.org/10.1016/j.ijpharm.2021.120426
Reference: IJP 120426

To appear in: *International Journal of Pharmaceutics*

Received Date: 25 October 2020
Revised Date: 17 February 2021
Accepted Date: 20 February 2021

Please cite this article as: L. Zhao, M. Orlu, G.R. Williams, Electrospun fixed dose combination fibers for the treatment of cardiovascular disease, *International Journal of Pharmaceutics* (2021), doi: https://doi.org/10.1016/j.ijpharm.2021.120426

Electrospun fixed dose combination fibers for the treatment of cardiovascular disease

Lixiang Zhao, Mine Orlu*, Gareth R. Williams*

UCL School of Pharmacy, University College London,
29-39 Brunswick Square, London, WC1N 1AX
* Corresponding authors: m.orlu@ucl.ac.uk ; g.williams@ucl.ac.uk

Abstract

Fixed dose combinations (FDCs) offer an accessible way to simplify complex therapeutic regimens by the simultaneous presentation of multiple drugs in a single entity to the patient. However, encapsulation of hydrophobic drugs into FDCs possess a number of technical challenges. Electrospun nanofibers offer a convenient way to incorporate multiple hydrophobic drugs into a single formulation in a single step, via the use of an appropriate organic solvent system during fabrication. In this study, we report a series of novel fiber formulations comprising ethyl cellulose loaded with two hydrophobic drugs, spironolactone and nifedipine, either individually or in combination. The drugs are found to be present in the fibers in the form of amorphous solid dispersions, and these are stable at room temperature for 4 months. The products showed extended release profiles over more than 30 h. This formulation strategy offers potential to manage chronic cardiovascular conditions and overcome patient related non-adherence by providing a simplified treatment model.

1. Introduction

Globally, cardiovascular disease (CVD) is the leading cause of death, and

thousands of people die from CVD every day. Based on a case-control study by Kjeldsen (2018), hypertension (high blood pressure) has been identified as the crucial risk factor for the majority of CVD patients. To ameliorate this risk, antihypertensive therapy is applied. Although the latter has resulted in major benefits to patients' lives, very few novel hypertensive drug formulations are being developed, and extensive research indicates that patient adherence to the required dosage regimen is a major problem (Hill, Miller and Degeest, 2011; Mancia *et al.*, 2013; Burnier and Egan, 2019). Adherence is a particular problem in the CVD setting considering patients are typically taking many medications simultaneously. To overcome this issue, fixed dose combinations (FDCs) containing multiple active pharmaceutical ingredients in a single dosage form have attracted much attention. These can provide improved therapeutic outcomes and reduced side effects over multiple single-drug medicines, as well as enhancing patients' adherence to medication (Prisant, 2002).

Combined prescriptions of spironolactone (SPR; Figure 1) and nifedipine (NIF; Figure 1) are given to patients suffering from resistant hypertension in clinical practice. SPR has been reported to contribute reducing the systolic blood pressure when added into the multiple antihypertensive treatment regimens (Takahashi *et al.*, 2015). SPR, a potassium-sparing diuretic, is a selective aldosterone antagonist (Wermuth, 2008). NIF is a calcium channel blocker for the treatment of hypertension and angina pectoris. Both SPR and NIF are Biopharmaceutics Classification System (BCS) Class II compounds with low solubility and high permeability, which raises a number of challenges for the development of effective oral dosage forms (Shamma and Elkasabgy, 2016). There is no available licensed patient-centric formulation incorporating both SPR and NIF (e.g. an easy to swallow oral suspension), leading to the use of individual suspension oral dosage foms of these drugs. An oral solid FDC of

SPR and NIF with a good stability profile would have the potential to improve adherence to the treatment regimen for the management of resistant hypertension.

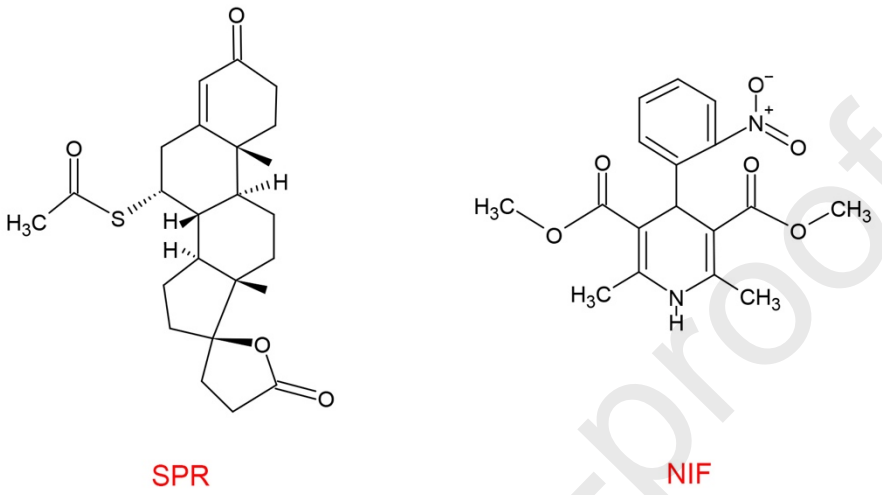

Figure 1: SPR and NIF chemical structures

FDCs have become widespread in the treatment of CVD in the last decade (Wan, Ma and Zhang, 2014). Traditional FDC manufacturing technologies include multilayer tablets, hot-melt extrusion, and active film-coating (Desai *et al.*, 2013; Vynckier *et al.*, 2014). An alternative approach which has recently begun to gain attraction is the electrospinning technique (Williams, Raimi-Abraham and Luo, 2018). This is a low-cost, versatile, and simple method resulting in the production of nanoscale fibers. The process functions by solidifying a solution through the application of electrical energy, and the rapid drying that ensues tends to yield products in the form of amorphous solid dispersions. The nanofiber formulations generated possess a high surface area to volume ratio, and can be prepared from many different polymers (Williams, Raimi-Abraham and Luo, 2018). Electrospun fibers have been applied in a range of areas, such as membranes/filters, tissue engineering, wound dressings, sensors, and in drug delivery (Xue *et al.*, 2017).

For poorly water-soluble drugs, electrospun systems are mostly employed to accelerate dissolution.Both the presence of the active ingredient in the amorphous state and the large surface area of the nanofibers can dramatically increase the rate of drug dissolution if a freely water-soluble polymer is used as the filament former (Sarfraz *et al.*, 2017; Williams, Raimi-Abraham and Luo, 2018). This has been shown for a wide range of drugs such as piroxicam (Paaver *et al.*, 2015), ibuprofen and carvedilol (Potrč *et al.*, 2015). Electrospinning has also been applied to generate fast-dissolving FDCs (Bukhary, Williams and Orlu, 2018).

Beyond fast dissolving systems, the use of insoluble polymers can result in electrospun sustained release drug formulations (Yu *et al.*, 2013; Li *et al.*, 2014; Um-i-Zahra *et al.*, 2014; Hu *et al.*, 2016; Lu *et al.*, 2017). Because the drug is usually amorphously distributed in the fibers, such systems act as diffusion controlled matrix formulations. In these, the rate of drug release is governed by how rapidly it moves through the polymer carrier, allowing significant control over the release profile through judicious choice of polymer. One suitable water-insoluble carrier polymer is ethyl cellulose (EC). EC has been widely used to achieve sustained release from electrospun formulations. For example, the antibiotic streptomycin showed a longer duration of antibacterial action when incorporated in to EC fibers than the bulk drug (Park, Kim and Lee, 2015). In other work, Li *et al* (2014) achieved sustained release of quercetin over 24 h period by loading into electrospun EC fibers. Huang's group (2020) designed a new kind of core-shell nanofibers through EC to achieve a sustained release effect of a model drug.

Electrospinning has previously been shown to be a suitable technique for

fabricating SPR and NIF formulations. For instance, Balogh's group (2017) developed solid dispersions of SPR in Eudragit® FS 100 through electrospinning and observed drug release over 2-4 hours. In other work, Lin, Tang and Du (2013) used electrospinning to formulate NIF-loaded nanofibers comprising polycaprolactone blended with polyurethane, which also exhibited sustained-release.

In this work, we used EC as a suitable polymer carrier in which to load SPR and NIF, with the aim of developing extended release formulations allowing once-daily dosing. We first formulated single drug-loaded fibers with different contents of active ingredients, and then combined the two drugs in FDCs. The morphology, physiochemical properties, and drug release performance of the fibers were all investigated in detail.

2. Experimental

2.1 Materials

Ethyl cellulose (EC, 48% ethoxy, 4 cP) and spironolactone (SPR) were supplied by Sigma-Aldrich Ltd. 1,1,1,3,3,3-hexafluoro-2-propanol (HFIP, ≥99.5%) was sourced from Acros Organics Ltd. Nifedipine (NIF) was provided by Cayman UK. Phosphate buffered saline (PBS, pH = 7.4) tablets were obtained from VWR Life Sciences. All other chemicals were analytical grade, and all water was deionized before use.

2.2 Preparation of electrospinning solutions

Solubility testing was initially carried out to determine the most appropriate solvent in which to co-dissolve all three components of the fibers (EC, SPR and NIF). Pure HFIP was found suitable for this, while other solvents explored could

not dissolve all three components to suitable concentrations. EC was dissolved in HFIP under magnetic stirring for 24 h at room temperature, to yield clear and homogenous solutions with a polymer concentration of 15% w/v. Blank EC fibers were prepared using this recipe. For drug-loaded fibers, one hour ahead of electrospinning SPR or NIF were added to give concentrations of 0.75, 1.5, 2.25, 3.75 and 6% w/v (Table 1). The FDC spinning solutions contained these concentrations of each drug; for example, the solution used to make M5 contained 6% SPR and 6% NIF. Solution viscosity was measured using a Bohlin Gemini 150 rotational rheometer (Malvern Instruments) at a shear rate of 200 s^{-1}. Solution surface tension was measured using a Delta-8 instrument (Kibron Inc.).

Table 1: Compositions of the spinning solutions and solid fiber formulations.

Drug concentration in solution (% w/v)[a]	*Drug concentration in single-drug fibers (% w/w)*[b]	*Formulation ID*		*Total drug concentration in FDC fibers (% w/w)*[c]	*Formulation ID*
		SPR	NIF		
0.75	4.8	S1	N1	9.1	M1
1.5	9.1	S2	N2	16.7	M2
2.25	13.0	S3	N3	23.1	M3
3.75	20.0	S4	N4	33.3	M4
6	28.6	S5	N5	44.4	M5

[a] In the FDC formulations, the solution concentration detailed is for each drug (e.g. M1 was prepared from 4.8 % w/v SPR and 4.8% w/v NIF).

[b] w/w drug concentration is the drug concentration in final product (e.g. SPR% in S1 is calculated as [100 x 0.75/(15+0.75)]≈ 4.8%)

[c] This total concentration is split 1:1 w/w between NIF and SPR; thus, M5 contains 22.2% w/w NIF and 22.2% w/w SPR .

2.3 Electrospinning

Spinning solutions (3.0 mL) were loaded into a 5 mL disposable plastic syringes (Terumo, MediSupplies UK) with care taken to ensure there was no air bubble formation. The syringe was then mounted on a 78-9100 C syringe pump (Cole

Parmer) or a KDS-100-CE syringe pump (KD Scientific). A 21G stainless steel dispensing needle (spinneret; inner diameter 0.51 mm, Nordson EFD) was fitted to the tip of the syringe. The positive electrode of an HCP 35-35000 high voltage DC power supply (FuG Elektronik) was then attached to the spinneret. The grounded electrode was connected to a 14.7 × 20 cm metal plate collector covered with aluminium foil. Initial optimisation experiments were performed in which the collection distance was varied from 15-20 cm, the diameter of the spinneret between 0.51, 0.61, and 0.84 mm (21 – 18G), the flow rate between 0.4-1 mL/h, and the applied voltage over the range 5-20 kV. Small samples of fibers were collected on glass slides and examined under a microscope to check the morphology, seeking to obtain linear fibres with no droplets or beads-on-string morphology. This led to the best results with a 21G needle, the collector situated 17 cm from the spinneret, the solution ejected from the syringe at a constant rate of 0.6 mL/h and 17 kV voltage applied. Using these optimal condition, 3 mL of fluid was dispensed. Electrospinning was carried out under ambient conditions (20 ± 3 °C and relative humidity of 35 ± 5%)

2.4 Scanning electron microscopy (SEM)

A small sample was cut from each fiber formulation, and mounted onto an aluminium SEM stub (TAAB Laboratories) with carbon-coated double-sided tape. The samples were then coated with a 20 nm gold sputter (Quorum Q150T) under argon. A Quanta 200F field emission SEM (FEI) connected to a secondary electron detector (Everheart-Thomley Detector- ETD) was used to generate SEM images of the materials. The diameters of the fibers were measured by using the ImageJ software version 1.49 (National Institutes of Health) to determine the size of objects at up to ca. 200 points of measurement, from three SEM images.

2.5 Differential scanning calorimetry (DSC)

DSC analyses of samples were performed on a Q2000 calorimeter (TA Instruments). Samples (ca. 4.0 mg) were prepared in T130425 Tzero hermetic aluminum pans (TA instruments) and sealed with pin-holed aluminium hermetic lids. Nitrogen gas was purged through the instrument at a flow rate of 50 mL min^{-1} throughout measurements. Samples were typically heated from 20 to 250 °C at 10 °C min^{-1}. Data were processed using the TA Universal Analysis software version 4.5 (TA Instruments).

2.6 Fourier transform infrared (FTIR) spectroscopy

FTIR spectra were obtained using a Spectrum 100 spectrometer (Perkin Elmer). The spectral data were analyzed with the Essential FTIR v3.10.016 software (Operant LLC). Data were collected over the wavenumber range from 650 to 4000 cm^{-1}, with resolution 1 cm^{-1} and 4 scans obtained per sample.

2.7 X-ray diffraction (XRD)

Samples were first mounted in an aluminium sample holder. XRD patterns were then collected using a MiniFlex 600 diffractometer (Rigaku) supplied with Cu-Kα radiation (λ= 1.5418 Å) at 40 kV and 15 mA. Samples were scanned at 0.5° min^{-1} over the 2θ range 3-60°.

2.8 *In vitro* release studies

In vitro drug release was quantified using the shaking method. Approximately 2.5 mg of the fiber sample under test was immersed in 10 mL of PBS in a 50 mL Duran bottle covered with parafilm to prevent evaporation. The dissolution study was performed in a Gallenkamp orbital shaker incubator at 50 strokes min^{-1} and 37 °C. Aliquots (200 µL) were collected at predetermined time points, and the release medium replenished with an equal volume of pre-heated fresh

medium to maintain a constant volume. The SPR and NIF concentrations in the aliquots were quantified by HPLC (1260 Infinity Series, Agilent Technologies, USA). Where needed, aliquots were diluted with PBS to bring the concentration into range of the calibration curve. Dissolution testing was performed under non-sink conditions. The maximum concentration of SPR and NIF reached 75 mg/l if all the drug came out of the N5/S5/M5 fibers (the solubility in water of NIF and SPR pure drugs are 5.9 mg/L and 22 mg/L respectively; the solubility in water of either NIF or SPR drugs loaded in fibers is roughly 200 mg/L). Experiments were performed in triplicate (n =3).

The drug loading was determined by chromatographic analysis, which was carried out on an Agilent Technologies 1260 Infinity II LC System. A Kinetex 5 µm EVO C18 LC 100 × 2.1 mm column (Phenomenex Inc) was used for the separation. The mobile phase was composed of a gradient of methanol and water (from 80:20 to 35:65 v/v), with the latter adjusted to pH 3.5 with formic acid. All samples were filtered through a 0.45 µm membrane filter to avoid any erroneous results from un-dissolved particulates, and degassed for 10 min. SPR and NIF show the best absorbance at 237 nm and 230 nm respectively in phosphate buffered saline (PBS; pH 7.4) through UV detector. Optimising the wavelength detection at 237 nm, where SPR can be detected at 11 min and NIF can be detected at 7.5 min. The ijecteion volume was 5 µL, a flow rate of mobile phase was 0.5 mL/min, and the column temperature 40 °C and a needle wash applied after each injection to improve the precision in HPLC.

2.9 Stability studies

All fibers were stored in a vacuum desiccator with silica gel as desiccant for 4 months at room temperuture, and then subject to analysis by DSC as detailed

in Section 2.5.

3. Results and discussion

3.1 Fiber mophology

In general, smooth and cylindrical fibers were successfully produced (Figure 2) with the optimised electrospinning parameters. No drug crystals were visible on the surfaces or outside the freshly prepared fibers, suggesting the formation of homogeneous solid dispersions. The exception is M5, where some small particles that may arise from drug crystallisation are seen. This is consistent with visual observations, where some precipiration was observed in the spinning solution during the fabrication process.

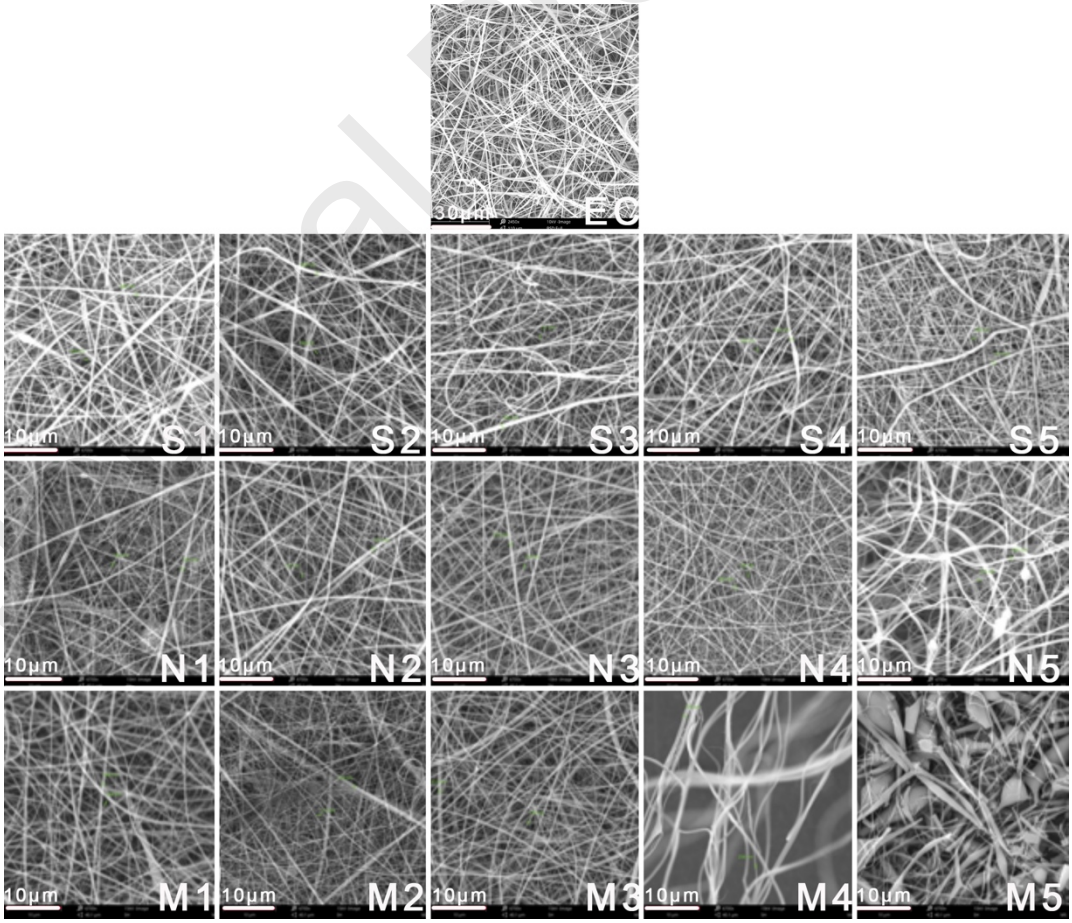

Figure 2: Morphological characterisation of the drug loaded fibers

*Working parameters: Voltage: 15kV; Magnify: 6700x; Area: 40.1μm *40.1μm

Fiber diameters were calculated from 200 SEM measurements, and are detailed in Figure S1 and Table S1 (Supplementary Information). The blank EC fibers have a mean diameter of 307 ± 31 nm. For the drug loaded formulations, the fibers with the lowest drug loading (S1, N1, and M1), have diameters slightly narrower than the blank EC formulation. The reduction in diameter results from an increase in the solution conductivity following the addition of SPR or NIF, which leads to more effective elongation of the polymer jet. This finding is in good agreement with data from other groups (Unnithan *et al.*, 2012; Li *et al.*, 2019). With an increasing drug loading there is an increase in the amount of mass expelled from the spinneret per unit time, and thus the fiber diameter is expected to rise. However this is balanced by changes in the viscosity and surface tension of the spinning solutions (see Tables S2-S4). There are no clear trends in viscosity or surface tension observed, and therefore a complex interplay beween solute content, viscosity and surface tension leads to there being no clear trends in the fiber diameters (Table S1). These factors also contribute to the formation of some beads in N5, and beading being very noticeable in M5, as well as to the observation of flattened fibers in M4.

3.2 Fourier-transform infrared spectroscopy (FTIR)

FTIR can allow us to understand how the drug molecules interact with polymer carrier, and thereby give insight into the likely stability of the formulation. The FTIR spectra are given in Figure 3. The fibers have virtually identical spectra to the EC material.

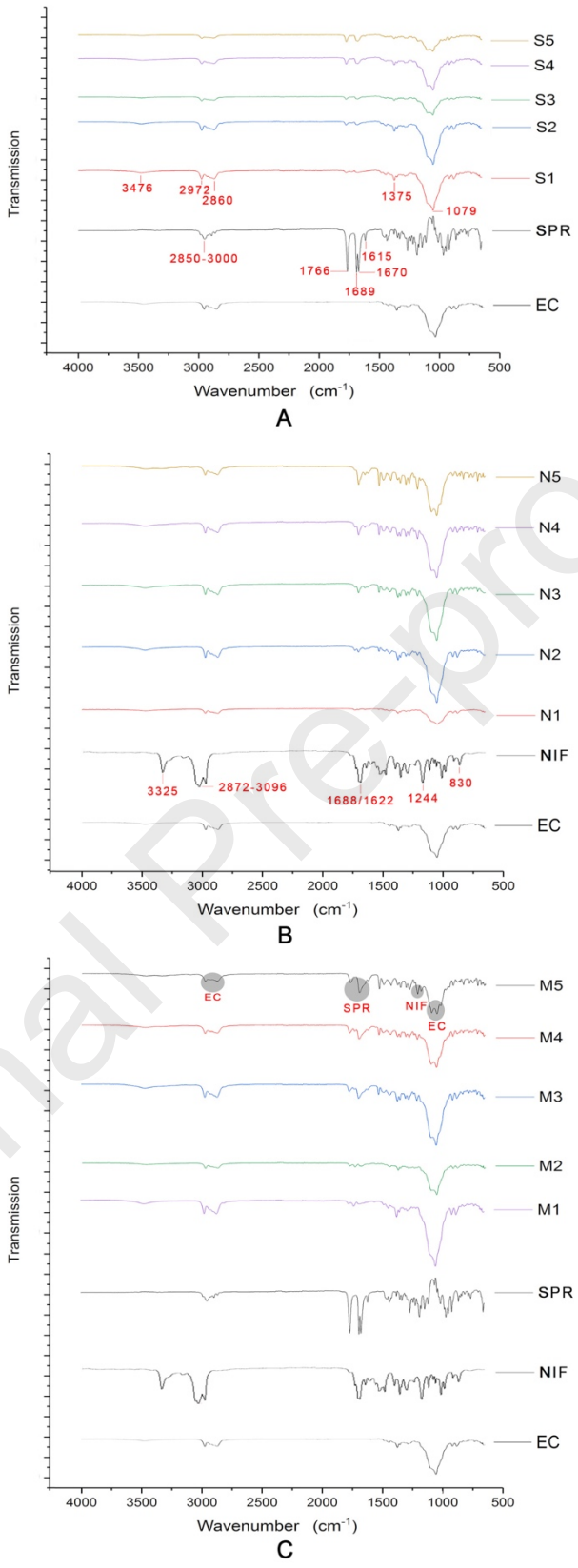

Figure 3: FTIR spectra of the raw materials and drug- loaded fibers, showing the (A) SPR, (B) NIF, and (C) FDC formulations.

EC has distinctive vibrations visible between 2860-2972 cm^{-1} (C-H stretching), and 1052 cm^{-1} (C-O ether bending). The spectrum of SPR shows C-H stretching between 2850-3000 cm^{-1}, C=O stretching from the γ-lactone ring at 1766 cm^{-1}, thioacetyl C=O stretching at 1689 cm^{-1}, a band from C=O in the ring at 1670 cm^{-1} and C=C stretching at 1615 cm^{-1} (Jafar *et al.*, 2015; de Resende *et al.*, 2016). NIF has characteristic peaks at 3325, 3096, 1688/1622, 1224 and 830 cm^{-1} representing amide stretching (N-H), aromatic group bands, aryl carboxylic group stretching vibration / pyridine group ring breathing band, carbonyl stretching, and C-N stretching of dihydropyridine (Li *et al.*, 2008; Alqurshi, Andrew Chan and Royall, 2017).

The drug loaded fiber products show IR spectra similar to blank EC fibers in Figure 3. However, with an increase of the drug loading, some carbonyl stretching vibrations from SPR and NIF emerge (e.g. at 1766 cm^{-1}, 1689 cm^{-1} and 1670 cm^{-1} from SPR, at 1688/1622 cm^{-1} from NIF). There are however some small shifts in peak positions observed, with for instance the SPR C-H bonds at ca. 2850-3000 cm^{-1} from SPR and the stretching vibration of the benzene ring in NIF between 2872-3096 cm^{-1} shifting position and broadening, presumably as a result of van der Waals interactions with the EC carrier (Lin, Tang and Du, 2013; de Resende *et al.*, 2016). Similarly the NIF N-H band at 3325 cm^{-1} has shifted to higher wavenumber and broadened considerably in the fiber products, suggesting H-bonding.

In the FDC fibers, the characteristic peaks of EC between 2860-2972 cm^{-1} and 1052 cm^{-1} can be clearly observed. The γ-lactone ring C=O group at 1766 cm^{-1}, the thioacetyl at 1689 cm^{-1}, and the 17 α-pregnene ring vibration at 1670 cm^{-1} from SPR can also be distinguished in the FDC formulation. The C-O vibration

of NIF at 1224 cm^{-1} was also observed in the higher loading FDC fibers. Again, some shifts in the position and intensity of the peaks can be observed indicating interactions between the drugs and EC carrier.

3.3 XRD

XRD was employed to characterize the physical form of SPR and NIF, EC, and the drug loaded fibers. The patterns are presented in Figure 4.

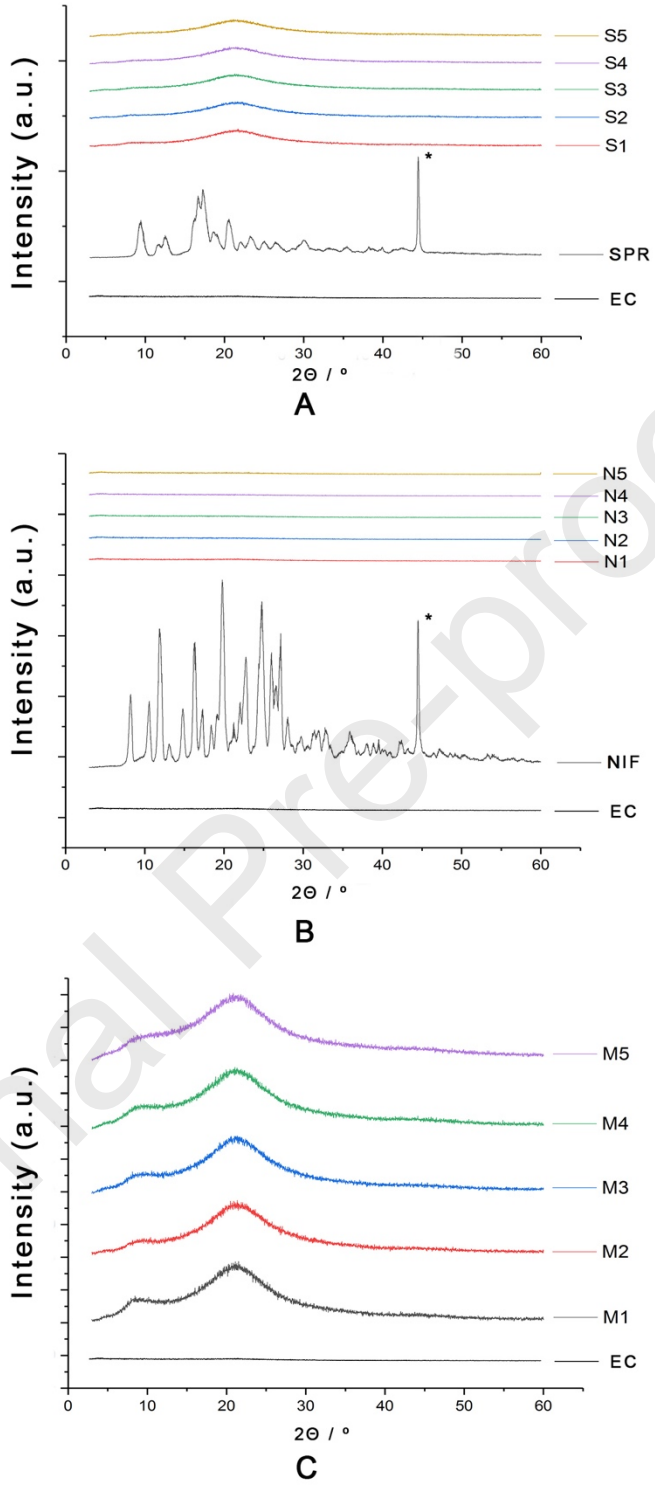

Figure 4: XRD patterns of SPR, NIF, and FDCs, showing the (A) SPR, (B) NIF, and (C) FDC formulations. * the peak at 44 degrees is from the Al sample holder

The SPR and NIF raw materials display numerous sharp reflections in their

XRD patterns. The characteristic diffraction peaks at 9.5°, 11.9°, 12.7°, 17.05°, 18.7°, 20.5°, 23.1°, 26.3°, 29.6°, and 35.4° for SPR and 8.12°, 11.81°, 16.25°, 19.63° and 24.47° with NIF reveal them to be the polymorphs SPR form II and NIF form I (Brown, Glass and Worthington, 2002; Grooff, Liebenberg and De Villiers, 2011; Da Silva Leite *et al.*, 2013; Jog and Burgess, 2018).

A broad halo can be observed at around 22° in the SPR and FDC formulations, while the NIF-loaded materials show no distinct features. In all cases and all drug loadings, the characteristic Bragg reflections of the raw active ingredients cannot be seen in the fibers' XRD patterns, consistent with their existing as amorphous solid dispersions, with no crystalline drug present.

3.4 DSC

DSC was used to verify the findings from XRD. Selected DSC thermograms are shown in Figure 5, with the remaining data and physical mixture are given in Figure S2 ans S5.

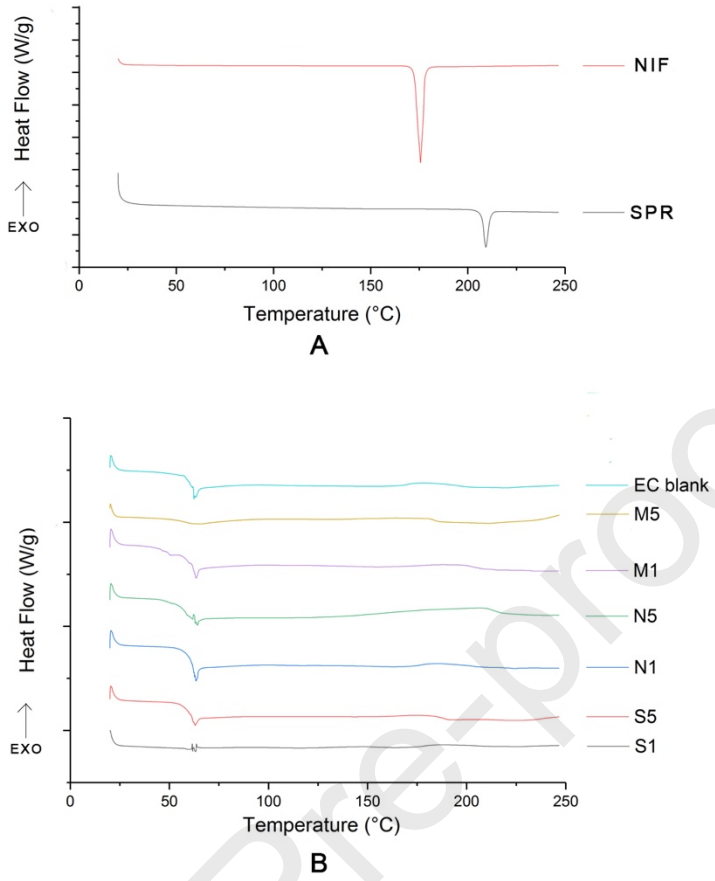

Figure 5: DSC analysis of (A) the pure drugs and (B) the formulations,

Distinct melting endotherms for SPR and NIF are observed at 207 °C and 175 °C respectively in Figure 5A. These agree well with the previous findings of Shamsuddin *et al.*, (2016) and Da Silva Leite *et al.*, (2013) who report the melting points of SPR form II to be 207 °C and 176 °C for NIF form I. The Inspection of the thermogram of the blank EC fibers reveals a melting peak at around 180 °C, as is consistent with the literature (Davidovich-Pinhas, Barbut and Marangoni, 2014). There is also an endothermic event visible at ca. 60 °C. This is superimposed on a baseline shift, meaning that it arises from the relaxation of amorphous material at the T_g (Quinten *et al.*, 2009). Thus, it appears that the EC material used in this work has two distinct T_gs, possibly because of the presence of chains of varied molecular weights.

For the drug loaded fiber formulations, the EC relaxation endotherm can be seen at around 60 °C in most cases. There is also a glass transition peak visible between 180 °C to 210 °C. However, in the fresh M4 and M5, due to the cross-linking of very dense drugs caused disruption of the segmental mobility, the glass transition peak at around 60 °C disappeared. Neither pure EC nor the drug loaded formulations show any phase transitions or fusion peaks in their DSC traces. This suggests that the drugs were present in the amorphous state, in agreement with the XRD results.

3.5 *In vitro* drug release studies

The drug loadings in the fibers were determined by HPLC and encapsulation efficiencies (EEs) are detailed in Table 2. In general, the EEs are close to 100%, except for the M5 fibers where values < 90% are noted. This arises due to recystallisation in the spinning solution, where some solid particles were observed to form. As expected, the actual content of SPR or/and NIF in most of products was equivalent to the 100% theoretical calculation value, suggesting no drug loss during the electrospinning process. In some cases, the reason of EEs >100% might be the inhomogeneous distribution of drugs, which caused by the long time still standing.

Table 2: The encapsulation efficiencies of the fiber products

Formulations	*Single drug loaded fibers*		*Fixed dosed combinations*	
	SPR (%)	*NIF (%)*	*SPR (%)*	*NIF (%)*
1	101.4 ± 0.7	99.8 ± 1.2	107.0 ± 0.8	108.6 ± 3.5
2	102.5 ± 1.2	102.8 ± 1.0	111.4 ± 4.7	111.7 ± 5.0
3	108.1 ± 2.5	101.4 ± 1.1	100.8 ± 1.4	102.8 ± 1.2
4	106.8 ± 1.7	107.4 ± 2.5	101.3 ± 1.3	102.5 ± 2.0

5	113.5 ± 3.9	103.2 ± 1.1	86.4 ± 2.3	87.7 ± 2.0

In vitro drug release studies were carried out in PBS at pH 7.4. The results are given in Figure 6, and the dissolution results on physical mixture of SPR, NIF pure drug and EC polymer were showed in Figure S6. The physical mixture shows no difference from the pure drugs on the drug release concentration.

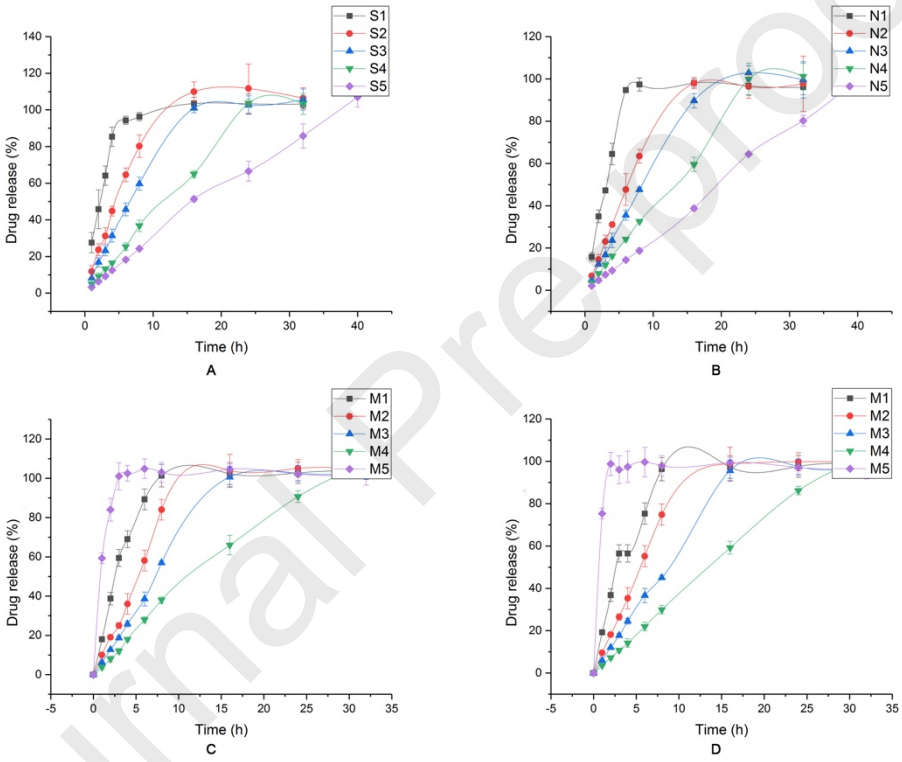

Figure 6: *In vitro* drug cumulative release profiles and three characterized drug release model. Data are shown as mean ± S.D. (n = 3). A) SPR loaded products, B) NIF loaded products, C) SPR release from FDCs, D) NIF release from FDCs

The formulations have a loading-dependent total release time in most cases. With an increase of the drug loading, the time taken to release 100% of the drug can be extended to more than 40 hours *in vitro* (it should be noted that elimination kinetics may reduce this time *in vivo*). A similar trend has been observed by other groups (Yu *et al.*, 2013). The exception here is M5, which gives much faster release than the other FDC formulations, for both SPR and

NIF. This might be a result of the different morphology of S5, where we see that beaded fibers with some drug particles at the surface have formed. In most cases, the drug release plots are close to being linear before the plateau in most cases, which augers well for extended release systems seeking to maintain a constant concentration of drug in the bloodstream. When control experiments were carried out using 1 mg of each pure drug or 1 mg of each SPR and NIF, almost zero drug release can be detected due to the slow dissolution rate and poor water solubility of both drugs.

The FDCs generated here achieved long-duration extended release, over which time the drugs could be absorbed in the human body to ensure a continued therapeutic effect (Sun and Lee, 2013). This is also the first study to combine SPR and NIF in a single formulation. Among the designed FDC formulations, M4 showed the maximum extended *in vitro* drug release profile. From a pharmacy practice point of view, FDCs are designed to present multiple APIs in a single entity to simplify administration and hence facilitate medicines management for chronic disease patients. The FDCs developed here have the potential to offer further advantages by providing sustained release of APIs, hence improving not only patient-related but also medicine-related adherence. Further studies should focus on comparing the effect of these FDCs on reducing adverse drug effects and on achieving long term clinical safety and efficacy for chronic therapies. Alternative polymers or fabrication routes could also be considered to determine the benefits and/or disbenefits of electrospinning as a fabrication route.

3.6 Stability studies

The fibers were stored for 4 months in a desiccator, after which DSC data were re-recorded in Figure 7, Figure S3). XRD data from the storage fibers possessed the same trand as the fresh ones (Figure S4).

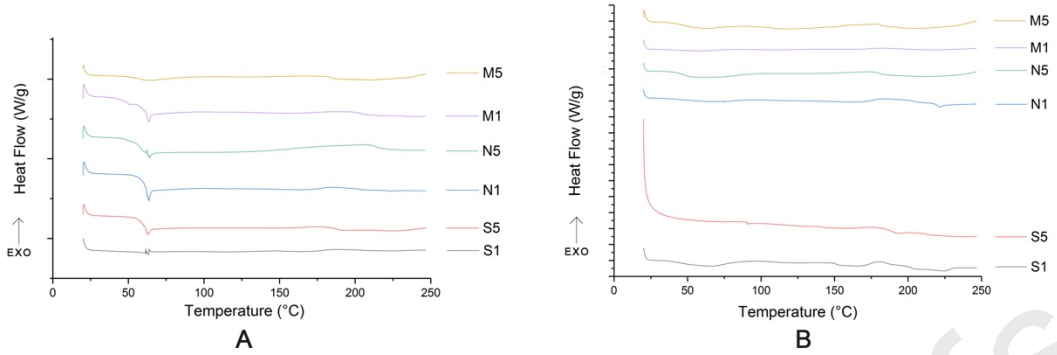

Figure 7: DSC analysis after 4 months desiccator storage.

A)Fresh products B)After 4 months storage products

Considering Figure 7, due to the long time stirage, S1, N5, M5 show a small endotherm from ca. 25 to 75 °C, which might arise from the adsorption of water in air. In all cases, a glass transition temperature is visible between 180 °C to 210 °C (Davidovich-Pinhas, Barbut and Marangoni, 2014). The lower-temperature T_g is also present, but the 60 °C relaxation endotherm of EC which was visible with the fresh fibers is no longer visible. The reasons for this are not clear, and this observation is counter-intuitive. What is clear is that no melting features in the form of endothermic peaks can be observed with any of the products, showing them to remain stable in the amorphous form over the storage period. In some cases, a degree of phase separation appears to have occurred. However, it is noteworthy that S5 exhibited an additional glass transition value at 92 °C. This value agrees well with a study from Jog and Burgess (2018), who reported the glass trasition temperature of SPR to be 91 °C. This suggests there might be some seperation of amorphous SPR from EC here. Overall the formulations remain stable without any recrystallization or phase seperation after 4 months of storage.

4. Conclusions

Monoaxial electrospinning was used in this work to prepare nanofiber

formulations loaded with spironolactone (SPR), nifedipine (NIF) and the two drugs together. Using ethyl cellulose as a carrier polymer we were able to generate drug-loaded nanofibers in the form of amorphous solid dispersions, which could give extended release at a virtually constant rate over up to 40 h. The total drug release time is mainly governed by the drug loading of the fiber formulations. The nanofiber products remained stable after 4 months storage at room temperature. This is the first study to develop sustained release solid state fixed dose combinations containing these poorly water soluble drugs for the treatment of hypertension. FDC platform should be considered for further research with the ultimate aim of providing patient-centric medicine for management of CVD diseases.

References

Akbari, J. *et al.* (2015) 'Improving the dissolution properties of spironolactone using liquisolid technique', *Pharmaceutical and Biomedical Research*. doi: 10.18869/acadpub.pbr.1.3.59.

Alqurshi, A., Andrew Chan, K. L. and Royall, P. G. (2017) 'In-situ freeze-drying-forming amorphous solids directly within capsules: An investigation of dissolution enhancement for a poorly soluble drug', *Scientific Reports*. doi: 10.1038/s41598-017-02676-2.

Balogh, A. *et al.* (2017) 'Controlled-release solid dispersions of Eudragit® FS 100 and poorly soluble spironolactone prepared by electrospinning and melt extrusion', *European Polymer Journal*. doi: 10.1016/j.eurpolymj.2017.08.032.

Brown, M. E., Glass, B. D. and Worthington, M. S. (2002) 'Binary systems of nifedipine and various cyclodextrins in the solid state. Thermal, FTIR, XRD studies', in *Journal of Thermal Analysis and Calorimetry*. doi: 10.1023/A:1016012407860.

Bukhary, H., Williams, G. R. and Orlu, M. (2018) 'Electrospun fixed dose formulations of amlodipine besylate and valsartan', *International Journal of Pharmaceutics*. doi: 10.1016/j.ijpharm.2018.08.008.

Burnier, M. and Egan, B. M. (2019) 'Adherence in Hypertension', *Circulation research*. doi: 10.1161/CIRCRESAHA.118.313220.

Davidovich-Pinhas, M., Barbut, S. and Marangoni, A. G. (2014) 'Physical structure and thermal behavior of ethylcellulose', *Cellulose*. doi: 10.1007/s10570-014-0377-1.

Desai, D. *et al.* (2013) 'Formulation design, challenges, and development considerations for fixed dose combination (FDC) of oral solid dosage forms', *Pharmaceutical Development and Technology*. doi: 10.3109/10837450.2012.660699.

Grooff, D., Liebenberg, W. and De Villiers, M. M. (2011) 'Preparation and

transformation of true nifedipine polymorphs: Investigated with differential scanning calorimetry and X-Ray diffraction pattern fitting methods', *Journal of Pharmaceutical Sciences*. doi: 10.1002/jps.22419.

Hill, M. N., Miller, N. H. and Degeest, S. (2011) 'Adherence and persistence with taking medication to control high blood pressure', *Journal of the American Society of Hypertension*. doi: 10.1016/j.jash.2011.01.001.

Hu, J. *et al.* (2016) 'Electrospun Poly(N-isopropylacrylamide)/Ethyl Cellulose Nanofibers as Thermoresponsive Drug Delivery Systems', *Journal of Pharmaceutical Sciences*. doi: 10.1016/S0022-3549(15)00191-4.

Huang, C. K. *et al.* (2020) 'Ethylcellulose-based drug nano depots fabricated using a modified triaxial electrospinning', *International Journal of Biological Macromolecules*. doi: 10.1016/j.ijbiomac.2020.02.239.

Jog, R. and Burgess, D. J. (2018) 'Nanoamorphous drug products – Design and development', *International Journal of Pharmaceutics*. doi: 10.1016/j.ijpharm.2018.10.046.

Kjeldsen, S. E. (2018) 'Hypertension and cardiovascular risk: General aspects', *Pharmacological Research*. doi: 10.1016/j.phrs.2017.11.003.

Li, C. *et al.* (2014) 'Tunable biphasic drug release from ethyl cellulose nanofibers fabricated using a modified coaxial electrospinning process', *Nanoscale Research Letters*. doi: 10.1186/1556-276X-9-258.

Li, H. *et al.* (2019) 'The effect of collection substrate on electrospun ciprofloxacin-loaded poly(vinylpyrrolidone) and ethyl cellulose nanofibers as potential wound dressing materials', *Materials Science and Engineering C*. doi: 10.1016/j.msec.2019.109917.

Li, P. *et al.* (2008) 'Chitosan-alginate nanoparticles as a novel drug delivery system for nifedipine', *International Journal of Biomedical Science*.

Lin, X., Tang, D. and Du, H. (2013) 'Self-assembly and controlled release

behaviour of the water-insoluble drug nifedipine from electrospun PCL-based polyurethane nanofibres', *Journal of Pharmacy and Pharmacology*. doi: 10.1111/jphp.12036.

Lu, H. *et al.* (2017) 'Electrospun water-stable zein/ethyl cellulose composite nanofiber and its drug release properties', *Materials Science and Engineering C*. doi: 10.1016/j.msec.2017.02.004.

Mancia, G. *et al.* (2013) '2013 ESH/ESC guidelines for the management of arterial hypertension: The Task Force for the management of arterial hypertension of the European Society of Hypertension (ESH) and of the European Society of Cardiology (ESC)', *European Heart Journal*. doi: 10.1093/eurheartj/eht151.

Paaver, U. *et al.* (2015) 'Electrospun nanofibers as a potential controlled-release solid dispersion system for poorly water-soluble drugs', *International Journal of Pharmaceutics*. doi: 10.1016/j.ijpharm.2014.12.024.

Park, J. Y., Kim, J. Il and Lee, I. H. (2015) 'Fabrication and characterization of antimicrobial ethyl cellulose nanofibers using electrospinning techniques', *Journal of Nanoscience and Nanotechnology*. doi: 10.1166/jnn.2015.10471.

Potrč, T. *et al.* (2015) 'Electrospun polycaprolactone nanofibers as a potential oromucosal delivery system for poorly water-soluble drugs', *European Journal of Pharmaceutical Sciences*. doi: 10.1016/j.ejps.2015.04.004.

Prisant, L. M. (2002) 'Fixed low-dose combination in first-line treatment of hypertension', in *Journal of Hypertension*. doi: 10.1097/00004872-200212000-00001.

Quinten, T. *et al.* (2009) 'Development of injection moulded matrix tablets based on mixtures of ethylcellulose and low-substituted hydroxypropylcellulose', *European Journal of Pharmaceutical Sciences*. doi: 10.1016/j.ejps.2009.02.006.

de Resende, R. C. *et al.* (2016) 'Analysis of spironolactone polymorphs in

active pharmaceutical ingredients and their effect on tablet dissolution profiles', *Brazilian Journal of Pharmaceutical Sciences*. doi: 10.1590/S1984-82502016000400005.

Sarfraz, R. M. *et al.* (2017) 'Application of various polymers and polymers based techniques used to improve solubility of poorly water soluble drugs: A review', *Acta Poloniae Pharmaceutica - Drug Research*.

Shamma, R. and Elkasabgy, N. (2016) 'Design of freeze-dried Soluplus/polyvinyl alcohol-based film for the oral delivery of an insoluble drug for the pediatric use', *Drug Delivery*. doi: 10.3109/10717544.2014.921944.

Shamsuddin *et al.* (2016) 'Development and evaluation of solid dispersion of spironolactone using fusion method', *International Journal of Pharmaceutical Investigation*. doi: 10.4103/2230-973x.176490.

Da Silva Leite, R. *et al.* (2013) 'Evaluation of thermal stability and parameters of dissolution of nifedipine crystals', *Journal of Thermal Analysis and Calorimetry*. doi: 10.1007/s10973-012-2605-y.

Sun, D. D. and Lee, P. I. (2013) 'Evolution of supersaturation of amorphous pharmaceuticals: The effect of rate of supersaturation generation', *Molecular Pharmaceutics*. doi: 10.1021/mp400439q.

Takahashi, F. *et al.* (2015) 'Successful treatment with an antihypertensive drug regimen including eplerenone in a patient with malignant phase hypertension with renal failure', *Internal Medicine*. doi: 10.2169/internalmedicine.54.4425.

Um-i-Zahra, S. *et al.* (2014) 'Study of sustained release drug-loaded nanofibers of cellulose acetate and ethyl cellulose polymer blends prepared by electrospinning and their in-vitro drug release profiles', *Journal of Polymer Research*. doi: 10.1007/s10965-014-0602-5.

Unnithan, A. R. *et al.* (2012) 'Wound-dressing materials with antibacterial activity from electrospun polyurethane-dextran nanofiber mats containing

ciprofloxacin HCl', *Carbohydrate Polymers*. doi: 10.1016/j.carbpol.2012.07.071.

Vynckier, A. K. *et al.* (2014) 'Hot-melt co-extrusion for the production of fixed-dose combination products with a controlled release ethylcellulose matrix core', *International Journal of Pharmaceutics*. doi: 10.1016/j.ijpharm.2014.01.028.

Wan, X., Ma, P. and Zhang, X. (2014) 'A promising choice in hypertension treatment: Fixed-dose combinations', *Asian Journal of Pharmaceutical Sciences*. doi: 10.1016/j.ajps.2013.12.005.

Wermuth, C. G. (2008) *The Practice of Medicinal Chemistry*, *The Practice of Medicinal Chemistry*. doi: 10.1016/B978-0-12-374194-3.X0001-7.

Williams, G. R., Raimi-Abraham, B. T. and Luo, C. J. (2018) *Nanofibres in Drug Delivery*, *Nanofibres in Drug Delivery*. doi: 10.2307/j.ctv550dd1.

Xue, J. *et al.* (2017) 'Electrospun Nanofibers: New Concepts, Materials, and Applications', *Accounts of Chemical Research*. doi: 10.1021/acs.accounts.7b00218.

Yu, D. G. *et al.* (2013) 'Electrospun biphasic drug release polyvinylpyrrolidone/ethyl cellulose core/sheath nanofibers', *Acta Biomaterialia*. doi: 10.1016/j.actbio.2012.10.021.

Credit Author Statement_IJP-D-20-02958

Lixiang Zhao: Conceptualization, Methodology, Investigation, Formal analysis, Validation, Writing- Original draft preparation; **Mine Orlu:** Conceptualization, Formal analysis, Supervision, Writing- Reviewing and Editing; **Gareth R. Williams:** Conceptualization, Formal analysis, Supervision, Writing- Reviewing and Editing

Credit Author Statement_IJP-D-20-02958

Lixiang Zhao: Conceptualization, Methodology, Investigation, Formal analysis, Validation, Writing- Original draft preparation; **Mine Orlu:** Conceptualization, Formal analysis, Supervision, Writing- Reviewing and Editing; **Gareth R. Williams:** Conceptualization, Formal analysis, Supervision, Writing- Reviewing and Editing